JOURNAL OF SPACECRAFT AND ROCKETS
Vol. 29, No. 6, November-December 1992

Ground Verification of Deployment Dynamics of Large Deployable Space Structures

Akira Meguro* and Jin Mitsugi*
NTT Radio Communications Systems Laboratories, Kanagawa, Japan

This paper describes a precise verification procedure for antenna-deployment mechanisms using ground-deployment test data. Ground-deployment tests are carried out for a communication antenna reflector for the Engineering Test Satellite VI (ETS-VI). The antenna-deployment mechanism studied consisted of a bearing, a helical spring, a chassis, and a latch mechanism. The characteristics of individual parts were measured under space and ground conditions. Then the initial characteristic of a deployment mechanism is statistically predicted. Ground verification of a deployment mechanism is usually difficult because of atmospheric and gravitational effects especially at the system level. Therefore, a new verification procedure is employed. Two kinds of suspending system are developed to compensate for gravity effects. The characteristics of a deployment mechanism can be estimated by identifying system parameters for the equation of deployment motion. This estimation procedure covers all development stages, so that a characteristic history of a deployment mechanism can be easily obtained. Atmospheric and gravitational effects on deployment motion are taken into account as system parameters. It is clarified that all mechanical parts retain their initial characteristics during assembly and environmental testing.

Nomenclature

F_g = weight of the wing structure
F_i = tension of the ith wire in Fig. 8
f = generalized external force
I = moment of inertia of the wing structure about the hinge axis
k = spring constant
n = number of sampling data
$\bar{q}$ = system parameter vector
T = tension of wire in Fig. 9
T_a = air drag torque
T_d = initial driving torque
T_f = initial constraint torque
T_0 = sampling interval
t = deployment time
X, Y, Z = inertial coordinate system in Fig. 9
X', Y', Z' = wing structure fixed coordinate system in Fig. 9
X_L, Y_L, Z_L = center of gravity of the wing structure in the local coordinate system in Fig. 6
x_g, y_g, z_g = center of gravity of the wing structure in antenna reflector test coordinates in Fig. 8
x_i, y_i = coordinates of suspension points on the wing structure
x_{sw}, y_{sw}, z_{sw} = suspension point on test fixture in XYZ coordinates
x_{s1}, y_{s1}, z_{s1} = suspension point on wing structure in XYZ coordinates
α_i = inclination angle of the ith wire in the xy plane
α, β = inclination angles of deployment axis around X, Y axes, respectively
$\Delta F_{ix}, \Delta F_{iy}$ = variations of tension of the ith wire in x, y directions
$\Delta x, \Delta y$ = displacement of wire suspending points from the deployment axis
$\Delta\psi_x, \Delta\psi_y$ = inclination of deployment axis against gravity direction
$\Theta, \dot{\Theta}, \ddot{\Theta}$ = generalized displacement, velocity, the second derivation of Θ, respectively
θ = deployment angle

Received May 13, 1991; revision received April 16, 1992; accepted for publication April 20, 1992.

*Research Engineer, Communication Satellite Technology Laboratory. Member AIAA.

Introduction

ON-ORBIT deployment of large communication antennas is a critical technology for present and future economical satellite communication systems. Advanced satellite communication experiments will be conducted in 1993 using the engineering test satellite ETS-VI. A large-capacity, multibeam communication experiment requires high precision, large-scale onboard antenna reflectors. Two reflectors are stowed and secured against a truss structure during launch. The smaller transmit reflector is a solid dish, whereas the large receive reflector is composed of three pieces of shells. Each shell element has a mechanical axis around which the element rotates assisted by spring torque until it is locked into the predetermined position. Therefore, on-orbit deployment of the two communication antennas is the most critical event. Design and test methods for optimizing the antenna-deployment mechanisms are the key technologies to realize future satellite communication systems.

The following verification items have been studied in recent papers on deployment mechanisms: 1) measurement of deployment time and final deployment velocity; 2) prediction of in-orbit deployment dynamics; 3) prediction of in-orbit deployment reliability; and 4) measurement of in-orbit deployment performance. These items, however, are insufficient to develop accurate deployment characteristics. The first two items are mentioned in most reports about ground-deployment testing as the main criteria. For example, ground testing results for the 20/30 GHz antenna reflectors on the OLYMPUS satellite, which has similar deployment configurations to ETS-VI,[1,2] have been reported. The antenna tip hinge mechanism (ATHM) was employed to overcome the limits of the launcher's shroud or bay. To verify ATHM's deployment characteristics, deployment tests at equipment (ATHM) level and antenna level (deployment of tips) were carried out. Resultant deployment time and deployment velocity were described. Ground tests are influenced, however, by the interaction between mechanical parts and gravity and atmosphere

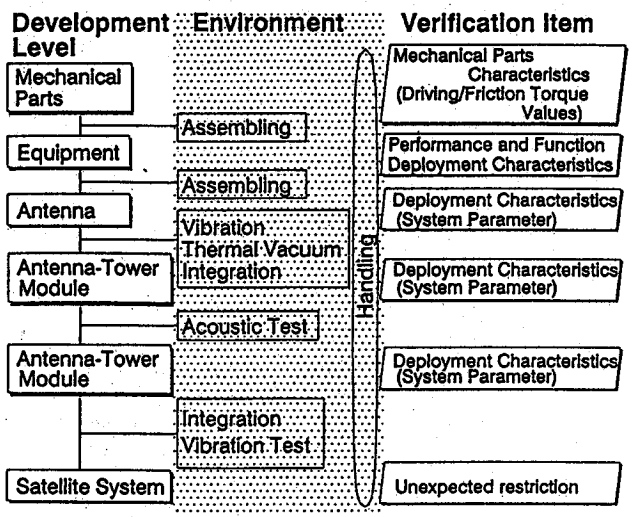

Fig. 1 Deployment test flow in ETS-VI program.

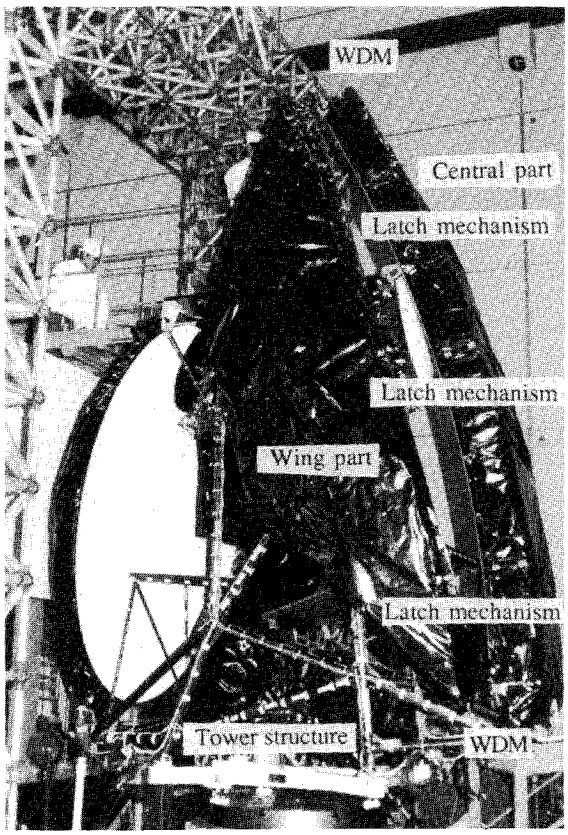

Fig. 2 ETS-VI antenna module.

effects. If these ground effects cannot be quantitatively estimated, the measured deployment time and velocity might differ from the actual values. In other words, even if the driving torque of the ATHM becomes weaker than the designed values, the measured values might happen to show a good agreement with the designed values due to the gravitational acceleration and the atmospheric deceleration.

Prediction of in-orbit deployment dynamics of INTELSAT VI transmission and receiving antennas have been reported.[3] In-orbit deployment is accomplished by a rotary negator spring mechanism with an integral viscous-fluid damping assembly. The deployment simulation of the receiving and transmission antenna system used both estimated and measured characteristics of individual mechanical parts. A statistical analysis has been proposed to predict the deployment dynamics of an antenna. The method is based on the driving and friction torque of mechanical parts whose statistical distributions fell within normal distributions.[4] In-orbit deployment reliability was verified with a probabilistic approach.

The deployment simulation of in-orbit motion is important for primitive design considerations and the prediction of in-orbit deployment reliability. However, the driving and friction torque may be changed by assembly and environmental testing. They must be verified by ground testing. In-orbit deployment performance of INTELSAT V communication antennas has also been reported.[5] Real-time telemetry from spacecraft sensors was used to evaluate the actual deployment motion. However, comparison between the telemetry data and the deployment characteristics was not described.

To realize the precise prediction of in-orbit deployment dynamics, a numerical evaluation method using mechanical parts characteristics gained from ground-deployment tests must be established. Precise gravity-compensation techniques and air-drag models are also necessary, especially at the antenna reflector level and the satellite system level.[6,7] This study introduces a new approach to estimate system parameters of deployment motion using experimental time series data of deployment angle and angular velocity. Gravity-compensation errors and atmospheric effects are also clarified and excluded from these data, respectively. Furthermore, two gravity-cancellation techniques are applied to the wing deployment test.

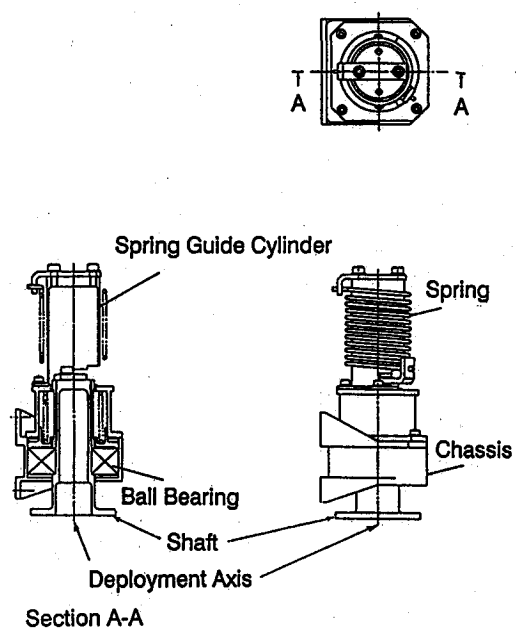

Fig. 3 Wing-deployment mechanism.

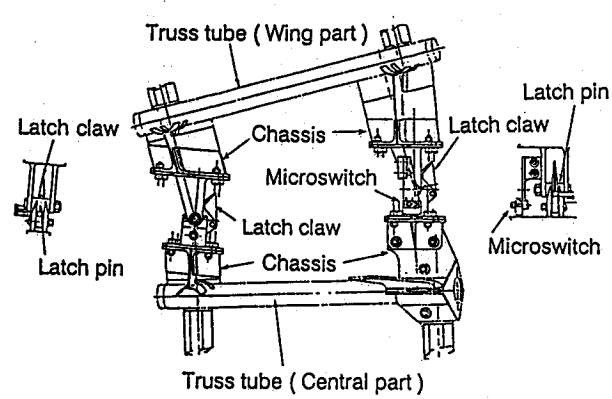

Fig. 4 Latch mechanism.

Table 1 Characteristics of mechanical parts

Item		Spring torque		Constraint torque	
		Stowed	Deployed	Stowed	Deployed
+ Y wing	Mean value, Nm	2.475	1.441	0.186	0.100
	Standard deviation, Nm	0.144	0.092	0.055	0.058
− Y wing	Mean value, Nm	2.733	1.682	0.128	0.107
	Standard deviation, Nm	0.098	0.089	0.071	0.056

Deployment Test Program

Figure 1 shows the deployment test steps in the ETS-VI program. Ground testing is composed of several test programs. Each program is performed at five development levels: mechanical parts level, equipment level, antenna assembly level, antenna-tower module level, and satellite system level. When the test programs advanced one step, the deployment mechanism (or mechanical parts) must encounter assembly and environmental testing. Assembly and environmental testing may affect the characteristics of the deployment mechanism (or mechanical parts). Therefore, deployment testing must be performed at each development level. Verification items corresponding to the development levels are limited to system configuration. For example, the exact simulation of on-orbit motion is significantly inhibited due to prominent gravitational and atmospheric effects at antenna assembly level, antenna-tower module level, and satellite system level. Thus, we must consider the optimum testing method for each development level. In this study, three methods for ground-deployment testing are described.

Antenna-Deployment Mechanism

Mechanism Description

ETS-VI is to be a large-capacity multibeam communication satellite using 13 beams in the 20/30-GHz frequency band and five beams in the 2.6/2.5-GHz frequency band. It has two large deployable main reflectors and other two deployable subreflectors. The largest reflector, which is 3.5 m in diameter, is divided into three portions. The two small outer portions are folded and fixed to the tower structure during launch as shown in Fig. 2. The wing deployment mechanism (WDM) is installed in the upper and lower hinges. Each WDM consists of ball bearings, a helical spring, a spring guide cylinder, a deployment axis, and a chassis as shown in Fig. 3. Latch mechanisms are installed in the backup truss structure. Each latch mechanism consists of latch claw, latch pin, and chassis as shown in Fig. 4. The helical spring provides driving torque, which is specified so as to ensure complete deployment of the wing structure and minimize latching shock. The ball bearing, the spring guide cylinder, and the latch claws are lubricated with MoS_2 solid lubricant to minimize sliding friction. In addition, electrical sensor cables are bound to the wings, and resistive bending moments arise around the hinge axes on deployment.

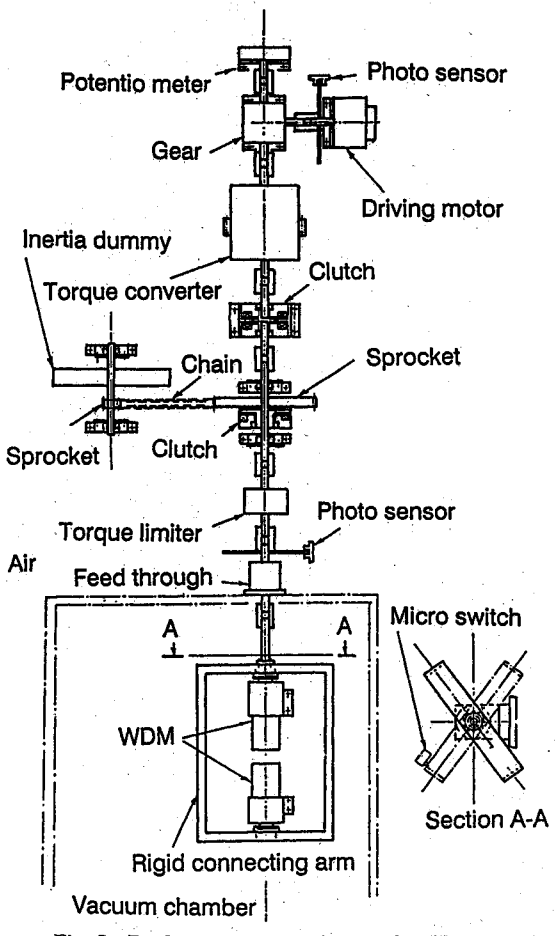

Fig. 5 Deployment test equipment for WDM.

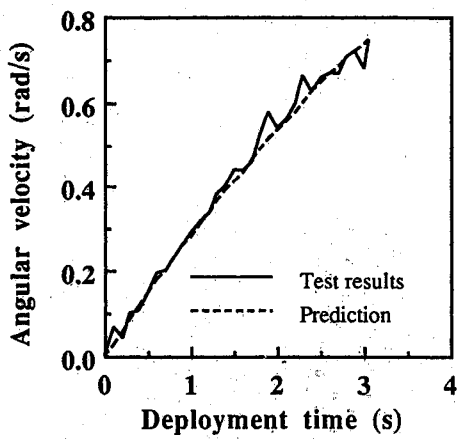

Fig. 6 Resultant angular velocity profile.

Mechanical Parts Characteristics

At the mechanical parts level, characteristics of mechanical parts were measured in several environmental conditions, considering the in-orbit and ground environments. Table 1 shows the values of the spring torque and the constraint torque of a pair of WDMs at room temperature and atmospheric condition. The constraint torque includes the rolling friction of the ball bearing, the sliding friction between the helical spring and the spring guidance cylinder, the constraint torque due to electrical sensor cables, and the latch claws. The high-constraint torque in the deployed position is mainly due to the latch claws. The spring and constraint torque of the WDM constituent parts will vary by virtue of manufacturing tolerances and materials variability.

Deployment Tests for Mechanism Equipment (Equipment Level)

Figure 5 shows the deployment test setup for a pair of WDMs. Low temperatures were achieved with a LN_2 refrigerator, whereas high temperatures were achieved with an electric line heater. A pair of WDMs were placed in the vacuum chamber, and the two deployment hinge axes were connected to each other by a rigid connecting arm. The deployment axis was led through the chamber wall. A magnetic fluid-type coupling sealed the vacuum chamber. To simulate the moment of inertia about the actual wing-deployment hinge axis, an inertia dummy was connected to the axis through a trans-

Table 2 Mass properties of the wing structure (nominal)

Center of gravity, m	$X_L = -0.051$	$Y_L = 0.44$	$Z_L = -0.16$
Moment of inertia, kg-m^2		3.5	
Mass, kg		10	

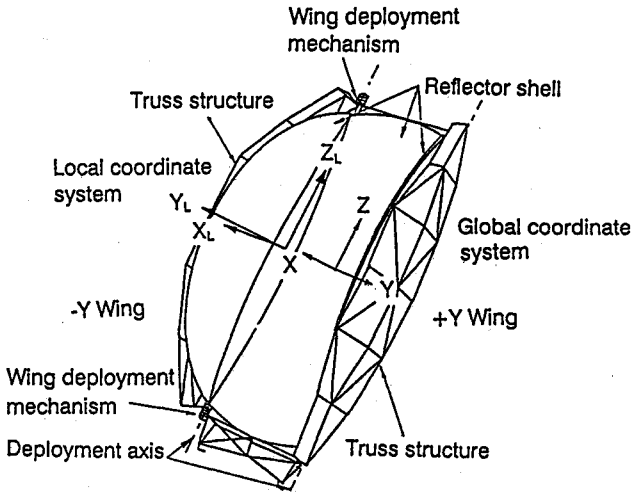

Fig. 7 3.5-m-diameter antenna reflector.

mission system. An angular measuring system was also connected to the hinge axis. An external driving system was connected to the hinge axis to measure the static reaction torque profile of the pair of WDMs prior to deployment testing. It was disconnected from the hinge axis when the deployment testing was performed. Resultant angular velocity profile at room temperature and atmospheric condition is shown in Fig. 6 as compared with analytically predicted angular velocity profile. The dynamic equation of deployment motion for the WDM equipment can be written as follows:

$$I\ddot{\theta} = T_d - k\theta - T_f - f\theta \tag{1}$$

The mean value of the stowed spring torque and the mean value of the stowed constraint torque are substituted into T_d and T_f, respectively. The spring constant and the constraint constant (the derivative from the stowed and deployed torque) are substituted into k and f, respectively, using Table 1. The angular profile can be obtained by initializing the system $\theta = \dot{\theta} = 0$ at $t = 0$.

The predicted profile shows good agreement with test results. It is primarily concluded that deployment characteristics can be evaluated precisely using mechanical parts characteristics.

Antenna Reflector Assembly

Structural Configuration

Figure 7 shows the structural configuration of the 3.5-m-diam antenna reflector (stowed configuration). It is composed of thin carbon fiber reinforced plastic (CFRP) skin honeycomb sandwich shells and a CFRP tube truss structure. The sandwich shell and the truss structure are connected to each other by adjustable studs to minimize surface error. Two WDMs are installed on each deployment axis to set the wing part. Twelve latch mechanisms are also installed along the mating plane in the truss structure to lock the wing in open position. The wing structure is stowed and secured against the truss tower structure during launch. Each wing structure is fixed at two points by explosive nuts. Mass properties of the wing structure are shown in Table 2.

Ground Deployment Test Facility

Gravity-Compensation Method

Ground-deployment testing is complicated by gravity and atmospheric effects. Gravity loading causes structural deformation and additional gravity torque on deployment. Gravity compensation is necessary to minimize external loading and latching shock on the deployment mechanism.

For the ground-deployment tests, gravity effects were canceled by suspending the wing structure. Figure 8 shows the deployment test setup for the antenna reflector assembly. The wing structure was set so that its deployment axis was vertical. The wing structure was suspended from two fixed points along deployment axes by wires. Five wires were used to cancel gravity effects on five degrees of freedom, except for rotation around the deployment axis. A potentiometer was installed on the deployment axis to measure instantaneous angle.

Setup Configuration Error

Figure 9 shows setup configuration errors. The most important errors are the inclination of deployment axes against gravity direction $\Delta\psi_x$, $\Delta\psi_y$, and the displacements of wire suspending points from the deployment axis Δx, Δy. Addi-

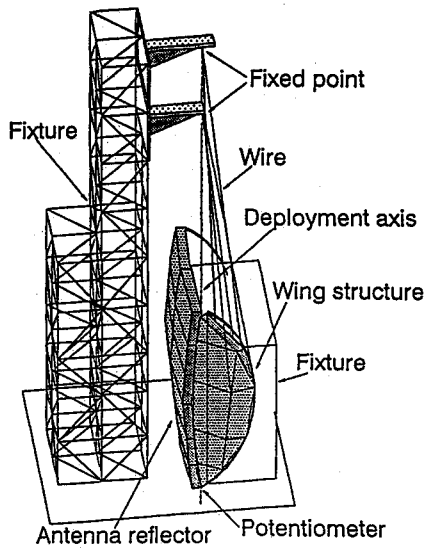

Fig. 8 Deployment test facility for reflector assembly.

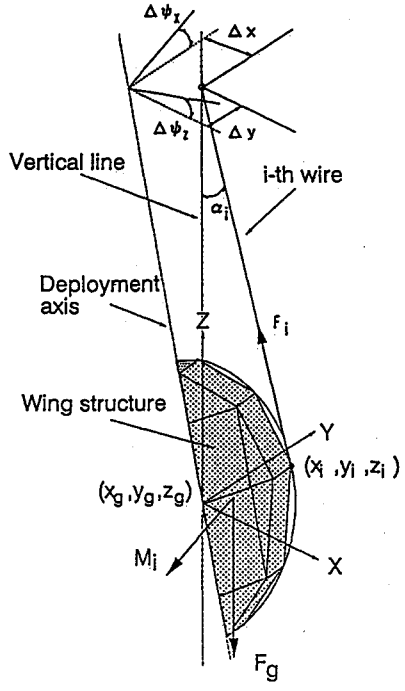

Fig. 9 Gravity-compensation error factors.

tional deployment moment due to setup configuration errors can be expressed[6] as

$$M_i = \left\{ \frac{\Delta x(F_i + \Delta F_{ix}) \cos \alpha_i \sin \theta}{\sqrt{x_i^2 + \Delta x^2 + 2x_i \Delta x \cos \theta}} + \frac{\Delta y(F_i + \Delta F_{iy}) \cos \alpha_i \sin \theta}{\sqrt{x_i^2 + \Delta y^2 + 2x_i \Delta y \cos \theta}} \right\} x_i + F_g x_g (\sin \Delta\psi_x \cos \theta + \sin \Delta\psi_y \sin \theta) \quad (2)$$

wire running over a pulley mounted on a freely revolving dish. A counter weight tensions the wire. The optimum setup conditions of the suspending system locations and wire tension are necessary to minimize geometry or force balance errors. Considering the additional moment due to gravity M_{og} and gravity-compensation moment M_{ot}, performance index G is defined to minimize compensation error as

$$G = \int_{\theta_0}^{\theta_f} (M_{og} + M_{ot})^2 \, d\theta = \int_{\theta_0}^{\theta_f} (AT + B)^2 \, d\theta \quad (4)$$

where

$$A = \left\{ \frac{x_{s1} - x_{sw}}{L_{sw}} (-\cos \beta \sin \theta) + \frac{y_{s1} - y_{sw}}{L_{sw}} (-\sin \alpha \cos \beta \sin \theta + \cos \alpha \cos \theta) + \frac{z_{s1} - z_{sw}}{L_{sw}} (\cos \alpha \sin \beta + \sin \alpha \cos \theta) \right\} \sqrt{x_{s1}^2 + x_{s1}^2}$$

$$B = -mg(\cos \alpha \sin \beta \sin \theta + \sin \alpha \cos \theta) \sqrt{x_{cg}^2 + y_{cg}^2}$$

Assuming that these errors are small compared to the height of the suspending point, these errors can be combined to the following approximate form using Taylor series.

$$a_1 \sin(a_2\theta + a_3) \quad (3)$$

Antenna Tower Module

System Layout

To stow the antenna reflector into the launch vehicle, the main reflectors are folded and inclined toward the tower structure. The wing-deployment axis, therefore, is inclined against the vertical line. The previous gravity-cancellation method is not applicable to this case. A new cancellation method was developed.

Ground Deployment Test Facility (Gravity Compensation)

Figure 10 shows schematic diagram of the wing-deployment test facility. It is very similar to the ground test facility of the wing reflector assembly, except for the inclination of the hinge axis. However, the wing reflector cannot be deployed without some form of gravity cancellation. The wing reflector is suspended by a single wire. The suspension system consists of a

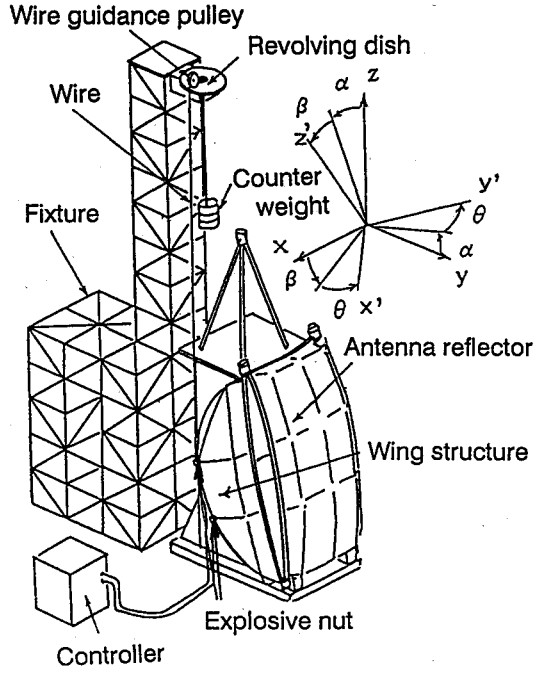

Fig. 10 Wing-deployment test facility.

Let suspending point coordinate (x_{sw}, y_{sw}, z_{sw}) and wire tension T be the system parameters in this function G. The first variation of the performance index is

$$\delta G = \frac{\partial G}{\partial T} \delta T + \frac{\partial G}{\partial x_{sw}} \delta x_{sw} + \frac{\partial G}{\partial y_{sw}} \delta y_{sw} \quad (5)$$

Optimum conditions are characterized by the stationary property of G.

Test Conditions and Error Estimation

Suspending point coordinates and wire tension were determined with respect to the setup conditions of the antenna reflector and mass properties of the wing structure. Table 3 summarizes these test conditions. Using these test conditions, the gravity-compensation error profile can be estimated analytically. It is shown in Fig. 11 as a function of deployment angle. In addition, the resultant optimum position of the upper suspension point will be located just above the suspension point on the wing structure when the wing structure is deployed in a gravity-stable position (where the gravity torque has zero value).

System Identification

Identification of Nonlinear System

The system equation of motion can be written in a general form as

$$\ddot{\Theta} = F(\Theta, \dot{\Theta}, \bar{q}, f, t) \quad (6)$$

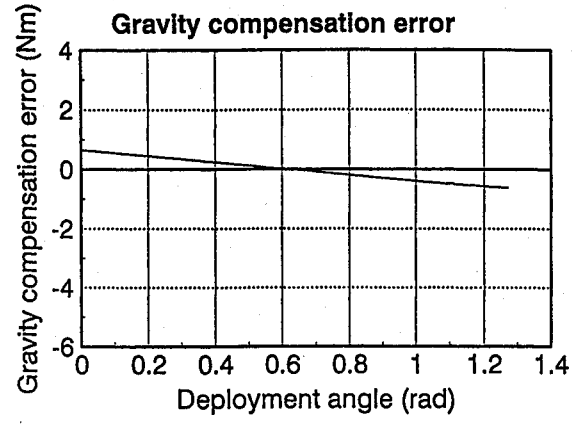

Fig. 11 Gravity-compensation error profile.

Table 3 Setup conditions

Item	Tension, N	Suspending point coordinate, m: Test facility	Wing structure
$+Y$ wing		$X=0.84$	$X=0.67$
	87	$Y=6.3$	$Y=1.4$
		$Z=0.020$	$Z=0.020$
$-Y$ wing		$X=0.84$	$X=0.68$
	88	$Y=6.4$	$Y=1.4$
		$Z=-0.05$	$Z=-0.05$

Table 4 Mean value of resultant system parameters (antenna assembly)

Item	System parameters q_1	q_2	q_3	q_4	q_5	q_6	q_7
$+Y$ wing	0.53	0.42	−0.64	0.00	0.0062	0.011	0.0012
$-Y$ wing	0.61	0.56	−0.33	0.00	0.034	0.0098	0.036

Table 5 Mean value of resultant system parameters (tower module)

Item	System parameters q_1	q_2	q_3	q_4	q_5	q_6	q_7
$+Y$ wing	0.50	0.46	−0.47	0.00	−0.90	0.61	−0.052
$-Y$ wing	0.60	0.44	−0.45	0.00	−1.31	−0.40	−0.11

Table 6 Characteristics of antenna reflector assembly

Item		Driving torque: Stowed	Deployed
$+Y$ wing	Average, Nm	2.384	1.284
	Standard deviation, Nm	0.097	0.234
$-Y$ wing	Average, Nm	2.806	1.276
	Standard deviation, Nm	0.072	0.364

Considering the n-component system parameter vector, a column matrix of a state of system degree of freedom is defined as

$$\bar{X}=\{x_1, x_2, \ldots, x_m\}=\left\{\Theta, \dot{\Theta}, \frac{\partial\Theta}{\partial q_1}, \frac{\partial\dot{\Theta}}{\partial q_1}, \ldots, \frac{\partial\dot{\Theta}}{\partial q_n}\right\} \quad (7)$$

The system equation of motion can then be rewritten as follows:

$$\frac{d\bar{X}}{dt}=\left\{x_2, \dot{F}, x_4, \frac{\partial\dot{F}}{\partial q_1}, \ldots, \frac{\partial\dot{F}}{\partial q_n}\right\} \quad (8)$$

A conventional numerical integration method (Runge-Kutta method) was used for solving the equation in discrete time series. The instantaneous states of system degree of freedom are then calculated. Using measured displacement at fixed intervals of time $\Theta_e(jT_0)$, performance index J is defined as

$$J=\sum_{j=0}^{n}\{\Theta(jT_0)-\Theta_e(jT_0)\}^2 \quad (9)$$

The first variation of the performance index J with respect to the system parameters is

$$\delta J=2\sum_{j=0}^{n}\{\Theta(jT_0)-\Theta_e(jT_0)\}\left\{\frac{\partial\Theta}{\partial q_1(jT_0)}+\cdots+\frac{\partial\Theta}{\partial q_n(jT_0)}\right\} \quad (10)$$

Simultaneous equations of system parameters are given as

$$\frac{\delta J}{\delta q_1}=2\sum_{j=0}^{n}\{\Theta(jT_0)-\Theta_e(jT_0)\}\frac{\delta\Theta}{\delta q_1}$$

$$\vdots \quad (11)$$

$$\frac{\delta J}{\delta q_n}=2\sum_{j=0}^{n}\{\Theta(kT_0)-\Theta_e(jT_0)\}\frac{\delta\Theta}{\delta q_n}$$

The steepest descent method or the Newton-Raphson method was employed to evaluate optimized system parameters.

System Dynamics

The system equation of the wing-deployment motion is obtained by adding Eq. (3) and the air-drag torque $-T_a$ to Eq. (1) as

$$I\ddot{\theta}=T_d-k\theta-T_f-f\theta-T_a+a_1\sin(a_2\theta+a_3) \quad (12)$$

This equation can be written in a generalized form as

$$\ddot{\theta}=q_1+q_2\theta+q_3\dot{\theta}^2+q_4\dot{\theta}+q_5\sin(q_6\theta+q_7) \quad (13)$$

Characteristics of Deployment Mechanism

Deployment characteristics were evaluated using both the deployment test data of the antenna reflector assembly and the antenna tower module. Both characteristics can be described by Eq. (12).

Tables 4 and 5 show resultant mean value of generalized system parameters of antenna reflector assembly and antenna tower module, respectively. Multiplying the moment of inertia by each parameter, we obtain the deployment parameters as shown in Table 6. These parameters are equivalent to deployment-mechanism characteristics. In Table 6, the standard de-

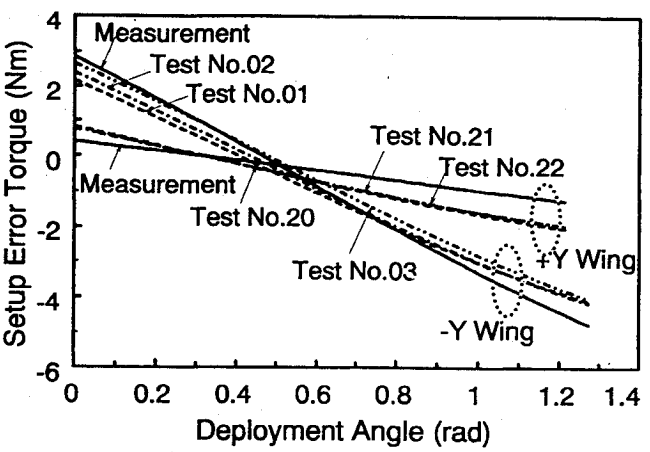

Fig. 12 Comparison between predicted and measured error profile.

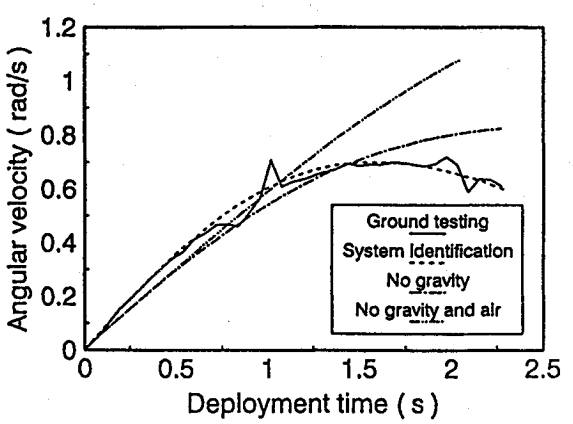

Fig. 13 Gravity and atmospheric effects on the deployment profile.

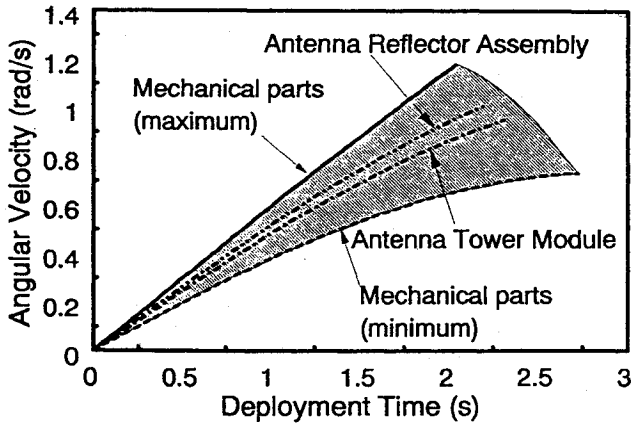

Fig. 14 Characteristics of deployment mechanism. (+ Y wing).

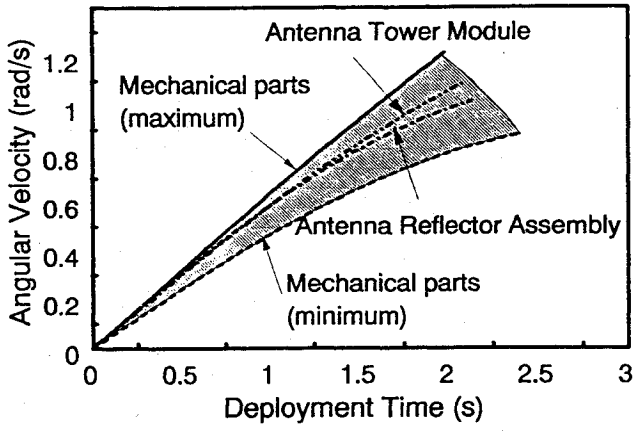

Fig. 15 Characteristics of deployment mechanism (− Y wing).

viation of the deployment torque in the deployed position is large as compared to initial mechanical parts characteristics (Table 1). The reason for this is that system parameter q_2 is affected by fluctuations in air loading and gravity-compensation errors.

The accuracy of these deployment parameters must be confirmed to verify the deployment-mechanism characteristics. First, a comparison of system parameters and setup error profile was performed. Figure 12 shows measured gravity-compensation error profile as compared with calculated profile using system parameters. The measured profile agrees with the calculated profile. Next, two system parameters of the deployment mechanism (q_1, q_2) were verified. Other parameters (q_3, q_4, q_5, q_6, q_7) are related to gravitational and atmospheric effects, and they were eliminated from the deployment profile to yield Fig. 13.

Figures 14 and 15 show the maximum and minimum deployment profiles, respectively. They were calculated using the characteristic distributions of mechanical parts. Resultant deployment profile of the wing structure, which is calculated using system parameters, is also indicated. The deployment range lies between maximum profile and minimum profile (hatched area). The hatched area shows a range of $\pm 3\sigma$ (standard deviation) predicted by the initial characteristics of individual parts. This means that the WDM maintains its initial deployment characteristics.

Conclusions

Ground-deployment tests for the antenna-deployment mechanism of the ETS-VI were performed with the object of verifying mechanical parts characteristics. In this study, they were estimated precisely by means of evaluating system parameters with a nonlinear equation of deployment motion using ground-deployment test results. Atmospheric effects, gravitational effects, and setup error were also estimated quantitatively by means of identifying system parameters related to atmospheric and gravitational effects. Ground testing results comprised of a range of $\pm 3\sigma$ (standard deviation) predicted by the initial characteristics of individual parts. It is clarified that the wing-deployment mechanisms of the communication antenna reflector for ETS-VI will maintain their design performance after undergoing testing and assembling.

References

[1]Stella, D., Morgant, F., and Nielsen, G., "Contraves Antenna Tip Hinge Mechanism for Selenia Sazio's 20/30 GHz Antenna," *Proceeding of the 2nd ESA Workshop on Mechanical Technology for Antennas,* European Space Agency, Paris, 1986, pp. 185–194.

[2]Martin, K., and De'Ath, D., "Evaluation from Hinge Actuator Mechanism to an Antenna Deployment Mechanism for Use on the European Large Communication Satellite (L-SAT / OLYMPUS)," *Proceeding of the 18th Aerospace Mechanism Symposium,* NASA, Scientific and Technical Information Branch, 1984, pp. 79–91.

[3]James, P. K., "Simulation of Deployment Dynamics for INTELSAT VI Transmit and Receive Boom/Antenna System," *COMSAT Technical Review,* Vol. 15, No. 1, 1985, pp. 127–141.

[4]Misawa, M., Yasaka, T., and Shojiro, M., "Analytical and Experimental Investigations for Satellite Antenna Deployment Mechanisms," *Journal of Spacecraft and Rockets,* Vol. 26, No. 3, 1989, pp. 181–187.

[5]Lomas, L., "In-Orbit Performance of INTELSAT V Communication Antennas Deployment System," *Proceeding of a Workshop on Mechanical Technology for Antennas,* ESA SP-225, Noordwijk, The Netherlands, Aug. 1984, pp. 133–139.

[6]Meguro, A., "Ground Testing Method for Large Deployable Antenna," *Proceedings of the 16th International Symposium on Space and Science,* AGNE Publishing, Tokyo, 1988, pp. 475–480.

[7]Meguro, A., "Considerations on Deployment Test Method for Large Satellite Antenna," *Proceedings of 1989 International Symposium on Antenna and Propagation,* Vol. 1, 1989, pp. 85–88.

Earl A. Thornton
Associate Editor